



Ultrafast exciton decomposition in transition metal dichalcogenide heterostructuresTomer Amit  and Sivan Refaely-Abramson *Department of Molecular Chemistry and Materials Science, Weizmann Institute of Science, Rehovot 7610001, Israel*

(Received 10 August 2023; revised 21 November 2023; accepted 4 December 2023; published 29 December 2023)

Heterostructures of layered transition metal dichalcogenides (TMDs) host long-lived, tunable excitons, making them intriguing candidates for material-based quantum information applications. Light absorption in these systems induces a plethora of optically excited states that hybridize both interlayer and intralayer characteristics, providing a distinctive starting point for their relaxation processes, in which the interplay between generated electron-hole pairs and their scattering with phonons play a key role. We present a first-principles theoretical approach to compute phonon-induced exciton decomposition due to rapid occupation of electron-hole pairs with finite momentum and opposite spin. Using the $\text{MoSe}_2/\text{WSe}_2$ heterostructure as a case study, we observe a reduction in the optical activity of bright states upon phonon scattering already in the first few femtoseconds after a photoexcitation, driving exciton interlayer delocalization and subsequent variations in the exciton spin. Our results reveal an unexpected and previously unexplored starting point for exciton relaxation dynamics, suggesting increased availability for coherent interactions and nonradiative processes through ultrafast changes in exciton momentum, spatial, and spin properties upon light excitation.

DOI: [10.1103/PhysRevB.108.L220305](https://doi.org/10.1103/PhysRevB.108.L220305)

Exciton relaxation processes underlying excited-state dynamics in heterostructures of transition metal dichalcogenides (TMDs) are a topic of broad interest [1–3]. The combination of optically active intralayer excitons, Coulomb-bound electron-hole pairs residing mainly within the individual layers, and low-lying interlayer excitons spread between the layers [4–8], induces relaxation mechanisms which are challenging to capture within simple frameworks. These involve a complex interplay between excitations with varying levels of layer and valley decomposition [9,10], determining spatial and spin properties that are directly coupled to system structure through the atomistic details of the participating layers and their relative alignment [11–13]. Gaining a comprehensive understanding of the involved excitonic processes and their structural dependencies is intriguing. In particular, considering variations in the excitonic nature along its time evolution subsequent to photoexcitation can guide design principles for effective generation of long-lived and ideally coherent exciton phases in TMD heterostructures [14–22].

A common approach to accurately describe structure-specific exciton properties is by constructing a solution in an excitonic basis set through the many-body Bethe-Salpeter equation within the so-called GW-BSE approach [23,24]. Within this first-principles framework, Coulomb and exchange interactions between multiple electron and hole wave functions are computed by numerically accounting for a large number of participating bands, with varying crystal momentum and spin properties, computed explicitly. This allows for an accurate consideration of dielectric effects, spin-orbit coupling, and exciton dispersion [25–28]. Further methodological advances enable computations of GW-based nonequilibrium effects on particle propagation by accounting for temporal evolution of the dielectric function and its consequences in time-resolved photoexcitation processes [29–34]. Still,

taking the wealth of participating particles into account in the relaxation processes is an extremely challenging task. Recent computational advances and theory developments allow predictive calculations of exciton scattering through phonons [35–38]. However, scattering with phonons can alter the internal exciton nature already at the single-exciton level [39]. Such effects can induce rapid changes in the exciton band composition and are thus expected to play a crucial role in the relaxation processes, in particular by modifying the optical selection rules that determine the cross play between exciton radiative recombination and nonradiative exciton-exciton scattering.

In this Letter, we present an *ab initio* computational scheme to compute ultrafast exciton decomposition following light excitation. We calculate the exciton time evolution upon coupling to phonons within a first-principles-based density matrix formalism, in which the electron-hole pairs composing the excitons scatter simultaneously, leading to time-resolved changes in the pair population. Demonstrated for the case of a $\text{MoSe}_2/\text{WSe}_2$ heterostructure, we show that such phonon-induced modifications in the electron-hole pair composition occur already within a few femtoseconds after excitation. These allow the occupation of momentum- and spin-indirect electron-hole pairs almost immediately, leading to instantaneous changes in the exciton oscillator strengths due to the induced layer delocalization and population of opposite-spin transitions. Our results demonstrate the delicate effects of ultrafast scattering events on the exciton properties, suggesting a new understanding of the starting point for exciton relaxation dynamics and shedding light on coherent coupling mechanisms between optically active intralayer excitons and long-lived interlayer excitons in TMD heterostructures.

We study the time evolution of optically excited low-energy interlayer and intralayer excitons in the $\text{MoSe}_2/\text{WSe}_2$ heterostructure with H_h^h layer alignment, schematically shown

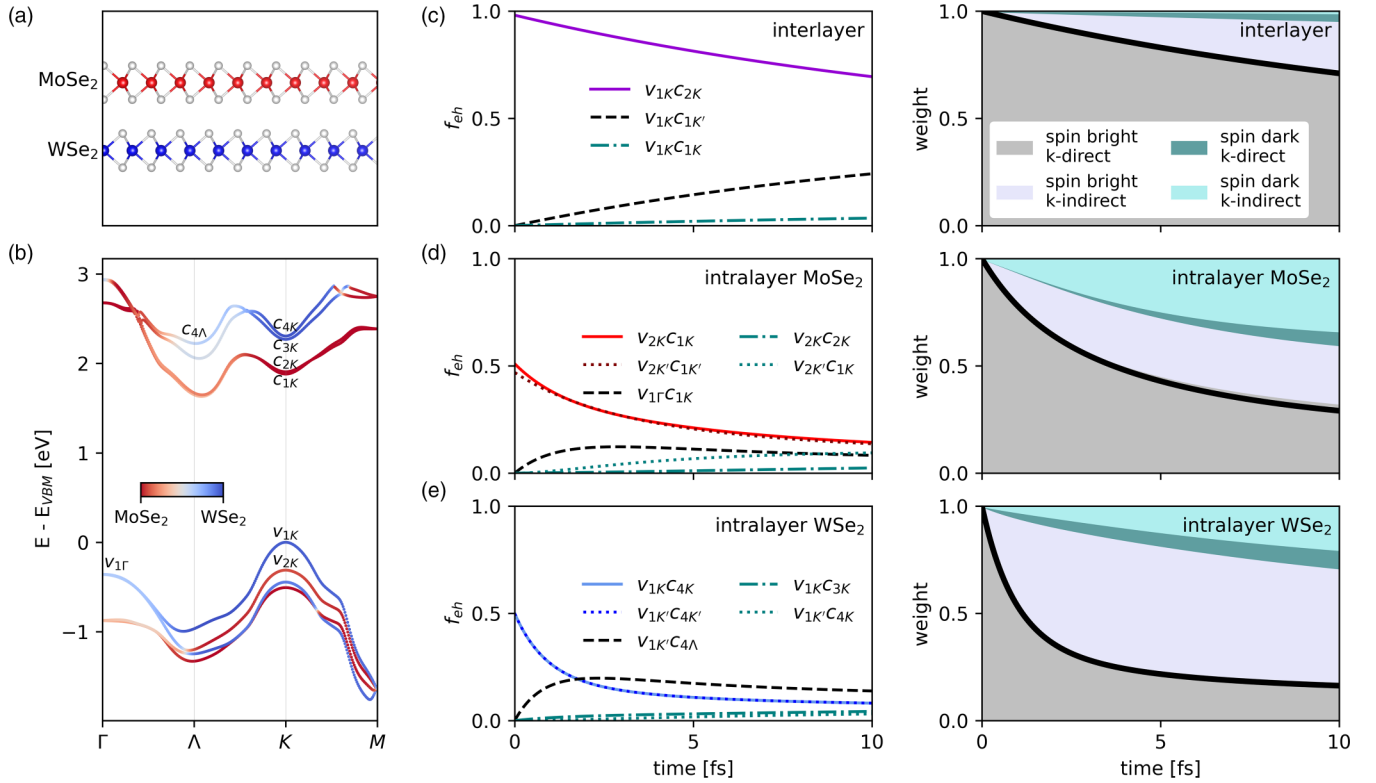


FIG. 1. Phonon-driven electron-hole pair decomposition of interlayer and intralayer exciton states in the MoSe₂/WSe₂ heterostructure. (a) Schematic representation of the examined TMD heterostructure of commensurate MoSe₂/WSe₂ in H_h stacking. (b) Electronic quasiparticle band structure computed within the GW approximation. Band colors represent the relative MoSe₂ (red) and WSe₂ (blue) layer contribution within the bands. Conduction (c) and valence (v) regions are shown with the notation of v_i, c_j for the highest valence and lowest conduction bands, respectively, and so forth. (c)–(e) Time-resolved evolution of three representative exciton states: interlayer, intralayer MoSe₂, and intralayer WSe₂. The initial occupation at time $t = 0$ represents the GW-BSE solution. Evolution of the relative electron-hole pair population in these excitons due to phonon scattering is shown in the center panels, for selected contributing pairs $v_{im}c_{jn}$ of holes and electrons at bands i, j and k points m, n , respectively. The right panels show the weighted pair occupation, summed over all participating transitions. The initially excited pairs are optically bright, with time-resolved population of momentum-indirect pairs, spin-dark pairs, and a combination of the two. Black line represents the relative optical transition probability upon pair decomposition.

in Fig. 1(a). Our starting point includes an electronic-structure evaluation of the electronic and excitonic states in this system, computed within the GW [23] and GW-BSE [24] approximation built on top of density functional theory (DFT) [40]. In this approach, exchange and screened Coulomb interactions between electrons and holes are computed through a full evaluation of the dielectric function and accounting for explicit wave-function coupling of both the spatial and spinor parts. At heterostructures, this procedure results with multiple optically excited states and absorption structure that strongly depends on the underlying heterostructure composition and alignment [10,11,41]. Phonon modes are computed within density functional perturbation theory (DFPT) [42], allowing a first-principles assessment of the participating electron-phonon and hole-phonon coupling (see Supplemental Material (SM) [43] for full computational details).

Figure 1(b) shows the calculated GW quasiparticle band structure, with band colors representing the relative wave-function contribution from the MoSe₂ (red) and WSe₂ (blue) layers. We first focus on the low-lying interlayer and intralayer exciton states, photoexcited around the K/K' valleys. The electron-hole transitions dominating the interlayer excitation are from the valence band (v_1), primarily localized on the

WSe₂ layer, to the conduction bands (a spin split of $c_{1,2}$), mainly localized on the MoSe₂ layer. Intralayer MoSe₂ transitions are primarily from the second valence band (v_2) to the conduction region, and intralayer WSe₂ transitions from v_1 to the higher-energy spin-split conduction bands ($c_{3,4}$). In the following we analyze the change in the electron-hole pairs composing these states and show that intralayer excitons inherent an interlayer nature already within a few femtoseconds upon coupling to phonons.

We compute the time evolution of the occupation of the electron-hole pairs composing the excitons in a Lindblad-type density-matrix representation [44–46] within a Liouville-von Neumann equation of motion, $\frac{\partial \hat{\rho}}{\partial t} = -\frac{i}{\hbar}[\hat{H}, \hat{\rho}]$. The systems Hamiltonian, $\hat{H} = \hat{H}_0 + \hat{H}'$, is composed of a noninteracting part, $\hat{H}_0 = \hat{H}_{eh} + \hat{H}_{ph}$, describing separately the pairs of electrons and holes (eh) composing the GW-BSE solutions and the phonon modes (ph) computed from DFPT. The interaction part, \hat{H}' , is perturbative and evaluated through electron (e)/hole (h)-phonon coupling, as we discuss below.

We define an initial state of an optically bright exciton, as computed from GW-BSE. This sets an initial density matrix that can generally be composed of the various participating

electron-hole pairs within the exciton basis set,

$$\hat{\rho}(t=0) = |S\rangle\langle S|$$

$$|S\rangle = \sum_{ehkQ} A_{ehkQ}^S |h, k\rangle |e, k+Q\rangle. \quad (1)$$

Here, $|S\rangle$ is an eigenstate solving the GW-BSE, with $|A_{ehkQ}^S|^2$ the probability amplitudes for each pair transition between holes (h) with crystal momentum k and electrons (e) with crystal momentum $k+Q$. The time propagation of the density matrix elements is computed by allowing each electron-hole pair (α_m) to interact independently with phonons, via

$$\frac{d\rho_{\alpha_i, \alpha_j}}{dt} = \frac{1}{2} \sum_{\alpha'_i \alpha'_j} [(\delta_{\alpha_i \alpha'} - \rho_{\alpha_i \alpha'}) P_{\alpha'_i \alpha'_j}^{eh} \rho_{\alpha'_i \alpha'_j} - (\delta_{\alpha'_i \alpha'} - \rho_{\alpha'_i \alpha'}) P_{\alpha'_i \alpha'_j}^{eh} \rho_{\alpha'_i \alpha'_j}] + \text{H.c.} \quad (2)$$

P^{eh} are scattering superoperators, $P_{eh_1 eh_2, eh'_1 eh'_2}^{eh} = P_{e_1 e_2, e'_1 e'_2}^e + P_{h_1 h_2, h'_1 h'_2}^h$, describing the electron-hole pair interactions with phonons. These superoperators are derived from the electron- and hole-phonon coupling terms, accounting for the temperature-dependent phonon occupation function and conserving the energy. For example, for the electron channel, $P_{e_1 e_2, e'_1 e'_2}^e = \sum_{\pm, \nu} B_{e_1 e'_1}^{\nu \pm} B_{e_2 e'_2}^{\nu \pm *} \delta_{m_1 h_1} \delta_{m_2 h_2}$, with $B_{e_1 e'_1}^{\nu \pm} = \sqrt{\frac{2\pi(n_{q\nu} + \frac{1}{2} \pm \frac{1}{2})}{\hbar}} g_{e_1 e'_1}^{\nu \pm} D_{e_1 e'_1}$, for $n_{q\nu}$ the Bose-Einstein occupation function for phonons with momentum q and mode ν , g is the particle-phonon coupling, \pm signifies phonon absorption (+) and emission (−), and D is an energy conservation function (see Supplemental Material (SM) [43] for full details). To reduce the computational effort we use a diagonal approximation in the propagation, although full matrix propagation leads to similar results for reduced k grids (see Supplemental Material (SM) [43]).

The underlying assumption for such interaction is that the optical exciton basis, generally composed of various electron-hole transitions energetically resonating together, can alter in the relaxation process. We thus explore the change in pair composition while allowing the hole and electron states to scatter into other bands through phonons. Room temperature is assumed throughout. In practice, this sets time-dependent changes in the occupation of the $|A_{ehkQ}^S|^2$ coefficients. While all initially occupied electron-hole pairs on the diagonal of $\hat{\rho}(t=0)$ are assumed to have momentum $Q=0$ within the optical excitation, upon phonon scattering, finite Q states become occupied, inducing layer mixing and allowing subsequent population of opposite-spin bands. This multistep propagation leads to rapid occupation of dark electron-hole transitions, effectively reducing the exciton optical transition probability, as we demonstrate below.

Figure 1(c), left panel shows the phonon-induced changes in the occupation f_{eh} of the main electron-hole (eh) pairs composing the interlayer exciton in the first ten femtoseconds following a photoexcitation. The initial occupation of the chosen state results from the v_1 to c_2 electron-hole transition at the K point, namely $v_{1K}c_{2K}$. Notably, the computed GW-BSE oscillator strength of this transition is only two orders of magnitude smaller than the optically active intralayer

excitons. This supports recent observations of optically allowed interlayer excitons in this systems [9,11,47]. The pair occupation is modified already in the first few femtoseconds due to a rapid intervalley transition into the $v_{1K}c_{1K'}$ pair (black dashed line). This transition is a result of electron-phonon interactions between the two spinlike conduction states, c_{2K} and $c_{1K'}$, at the opposite valleys K, K' . We note the difference between this phonon-induced ultrafast transition of exciton partial occupation and previously explored exchange-driven valley dephasing, expected to occur at longer timescales [48]. Following this transition, population of the pair $v_{1K}c_{1K}$ (teal dashed-dotted line) further occurs. This corresponds to an intravalley transition in which electrons scatter between the spin-split conduction bands c_{2K} and c_{1K} . This transition is somewhat unexpected, but easy to understand when considering the broken spinor symmetry in this structure, as we demonstrated in previous work [10,11], observed when using a periodic Bloch wave-function representation. This effect was previously shown to vary the exciton magnetic behavior [49–51]. Our calculations point to spin magnetic moment of $\langle S_z \rangle = -0.996$ and 0.980 for the c_{1K} and c_{2K} states, respectively, slightly breaking the naively expected values of ± 1.0 . The right panel summarizes the overall change in the electron-hole pair composition when summing over all participating pairs in the density matrix evolution. The initial pair occupation, momentum direct and spin bright by definition, quickly induces fractional population of momentum indirect and spin-dark contributions.

Figures 1(d), 1(e) show a similar analysis for two bright intralayer excitons, both dominating the corresponding peak regions in the computed absorption (see Supplemental Material (SM) [43]). In these states, the initial excitation is split between the two valleys (we note that this representation is invariant and can in general modify upon unitary transformation of degenerate solutions of the GW-BSE). Importantly, unlike the interlayer case, the immediate phonon relaxation of these states now includes transitions outside of the K/K' valleys. For example, for intralayer MoSe_2 , fast occupation of electron-hole pairs with the hole residing on the Γ point and the electron on the K/K' point are populated almost instantaneously (dashed black line). As an immediate, rather surprising result, this population follows with rapid occupation of pairs with dark spin (dashed teal lines). The corresponding substantial changes in the time-resolved weighted occupation of momentum-indirect and spin-dark states is shown in the right panel. We note that this fast occupation of optically dark states is a direct outcome of the participation of hole states at Γ in the density matrix scattering dynamics, a point in which the electron-hole spin number is ill defined. In the case of an initial intralayer WSe_2 exciton, rapid occupation of pairs with electrons residing at the Λ point dictates a large change in the momentum directness of the excited state, with population of indirect, optically dark transitions exceeding direct ones already within the first few femtoseconds. Again, these transitions further induce population of spin-flip states. These are slightly reduced compared to intralayer MoSe_2 upon the relatively conserved spin at the Λ point. We emphasize that these spin properties are highly sensitive to the band character, which can be structurally modified, for example, through interlayer twisting [10,12].

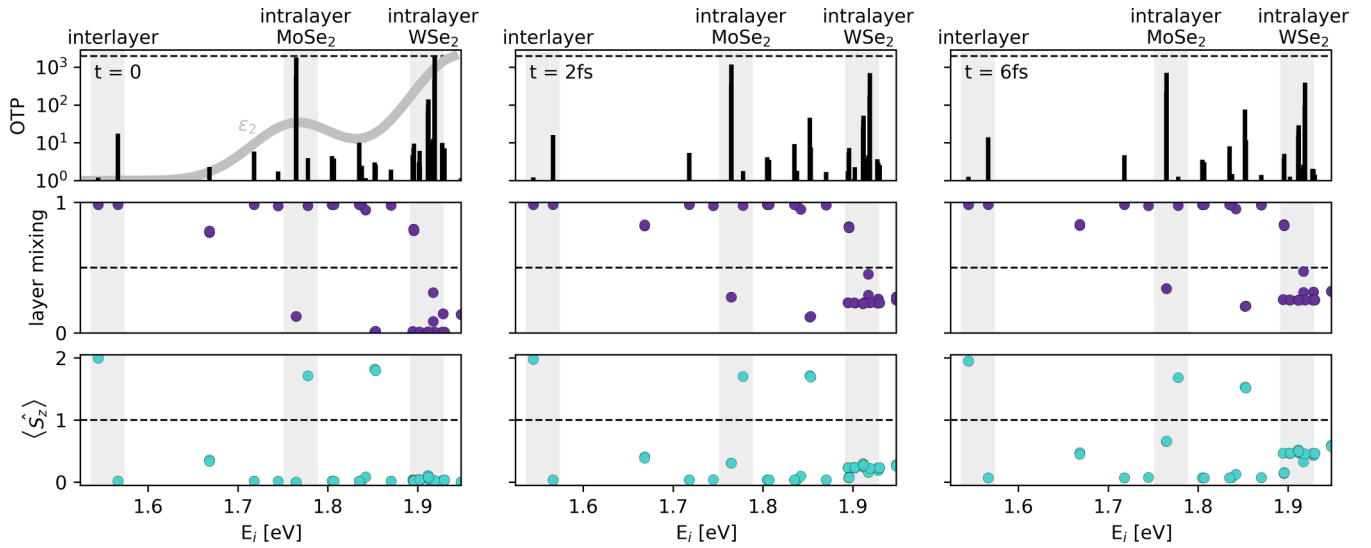


FIG. 2. Time-resolved evolution of the bright exciton states in the examined heterostructure. Top panels show the optical transition probability for each exciton in a logarithmic scale, computed through the optical transition probabilities of single electron-hole pairs and their varying relative contributions. The computed GW-BSE absorption spectrum at $t = 0$ is shown in the top left panel (gray line). Middle panels show the change in layer mixing for each state, with 0 representing fully intralayer and 1 representing fully interlayer excitons. Bottom panels show the corresponding out-of-plane spin expectation value for each state, where 0 stands for spinlike and 2 for spin-unlike exciton transitions. Reduction in the optical transition probabilities of the intralayer states occurs due to an increase in layer mixing, with associated population of spin-dark states, considerably modifying the starting point of the exciton relaxation dynamics.

While the above-chosen interlayer and intralayer states illustrate the origins of exciton decomposition in our approach, the computed GW-BSE absorption spectrum includes numerous bright excitations ranging between the interlayer and intralayer excitons, with varying initial compositions of electron-hole pairs (see Supplemental Material (SM) [43]). To capture the collective effect of the above-discussed time-resolved modifications, Fig. 2 shows the phonon-induced changes along this energy range. We specifically examine the time evolution of the exciton optical transition probability (OTP), calculated through the single-pair OTPs and their time-dependent populations; the level of layer mixing, where 0 stands for pure intralayer and 1 for pure interlayer states; and the out-of-plane spin expectation value $\langle \hat{S}_z | \hat{S}_z \rangle$, where 0 describes spinlike and 2 spin-unlike transitions. We present only initially bright states with computed oscillator strength $> 1 e^2 a_0^2$. The energy regions with the low-lying interlayer and intralayer states explored above are marked with gray shaded areas.

The immediate effect of the phonon-induced pair occupation is directly observed through the reduction in the OTP. This change is particularly visible at both intralayer regions, where the OTP of the brightest transitions is reduced by an order of magnitude. In addition, we note the immediate OTP reduction of states surrounding the main intralayer excitons, effectively suggesting a decreased broadening of these peaks. The associated changes in layer mixing and spin multiplicity demonstrate that these reductions in the OTP occur due to occupation of electron-hole pairs that enhance the interlayer nature of these excitons, involving states outside of the K, K' valleys.

The calculated pair decomposition and rapid layer mixing suggest that the excitons computed as photoexcited states in absorption can change within the relaxation. These obser-

vations supply a complementary view of recent findings by Paleari *et al.* [39], in which changes in the exciton state were computed upon simultaneous coupling of electrons, holes, and phonons within a self-consistent extended-BSE kernel, composing the so-called elemental excitons, as opposed to optical ones. Using the first-principles density matrix approach we presented here, and under the assumption of weak particle-phonon coupling, our findings offer an alternative view into the origins of these changes. We note that additional energy relaxation of the exciton state is expected to occur due to time-resolved modifications in the dielectric screening and corresponding changes in the electron-hole coupling. Such effects were recently studied in TMD monolayers for the nonexcitonic case [34], suggesting that these only become significant at longer timescales than the ones examined here. We further note that our results are still within a single-exciton framework; exciton-exciton interactions, not included here, are required to evaluate exciton decay lifetimes and spectral broadening comparable to experiment. Furthermore, such changes in the optical excitation nature due to phonon scattering directly point to modifications in their transport properties [38,52].

The presented approach for computing the exciton-phonon interaction dynamics is closely related to the common assumption that exciton-phonon scattering is primarily dominated by the static Fan-Migdal interaction terms, in which electron-phonon and hole-phonon coupling are weighted within the coupled exciton-phonon terms through GW-BSE state components [35]. While recent studies employed this approach to compute exciton-phonon scattering rates [36–38], our approach here is different: we keep the interactions within a single-exciton picture, but allow a change in the electron-hole pairs composing the excitons in the BSE basis set. The rapid layer mixing occurring directly after excitation of

intralayer states implies on effective coupling to long-lived interlayer excitons, and in practice suggests that many-body effects crucially contribute to the generation of ultrashort exciton coherences. We further note that although our method is fully from first principles, it treats phonons as a bath within a Markovian approximation, a property that can be challenged if one further accounts for changes in the phonon population [53]. We leave the numerical exploration of these multiparticle interactions to future work.

In conclusion, we presented a first-principles approach to compute exciton ultrafast dynamics through phonon-induced electron and hole pair occupation following an optical excitation. Our analysis, based on an *ab initio* density matrix formalism, points to a rapid reduction in the optical activity of intralayer excitons due to layer mixing. Furthermore, it suggests a new perspective of the starting point for the relaxation between optically excited intralayer states and long-lived in-

terlayer states, with spatial overlap between these excitons induced almost immediately after excitation, followed by occupation of spin-dark components. Our findings supply a structure-specific and state-dependent measure of the exciton decomposition following a photoexcitation, facilitating a predictive understanding of exciton relaxation due to phonon scattering from a band-structure perspective.

We thank Adva Baratz, Ouri Karni, and Uri Peskin for insightful discussions. S.R.A. acknowledges support from a Peter and Patricia Gruber Award and an Alon Fellowship. T.A. is supported by the David Lopatie Fellows Program. The project has received further funding from the European Research Council (ERC), Grant Agreement No. 101041159, and an Israel Science Foundation Grant No. 1208/19. Computational resources were provided by the ChemFarm local cluster at the Weizmann Institute of Science.

-
- [1] P. Rivera, H. Yu, K. L. Seyler, N. P. Wilson, W. Yao, and X. Xu, Interlayer valley excitons in heterobilayers of transition metal dichalcogenides, *Nature Nanotechnol.* **13**, 1004 (2018).
- [2] B. Müller, A. Steinhoff, B. Pano, J. Klein, F. Jahnke, A. Holleitner, and U. Wurstbauer, Long-lived direct and indirect interlayer excitons in van der Waals heterostructures, *Nano Lett.* **17**, 5229 (2017).
- [3] C. Jin, E. Y. Ma, O. Karni, E. C. Regan, F. Wang, and T. F. Heinz, Ultrafast dynamics in van der Waals heterostructures, *Nature Nanotechnol.* **13**, 994 (2018).
- [4] P. Rivera, J. R. Schaibley, A. M. Jones, J. S. Ross, S. Wu, G. Aivazian, P. Klement, K. Seyler, G. Clark, N. J. Ghimire, J. Yan, D. G. Mandrus, W. Yao, and X. Xu, Observation of long-lived interlayer excitons in monolayer MoSe₂-WSe₂ heterostructures, *Nature Commun.* **6**, 6242 (2015).
- [5] L. A. Jauregui, A. Y. Joe, K. Pistunova, D. S. Wild, A. A. High, Y. Zhou, G. Scuri, K. D. Greve, A. Sushko, C.-H. Yu, T. Taniguchi, K. Watanabe, D. J. Needleman, M. D. Lukin, H. Park, and P. Kim, Electrical control of interlayer exciton dynamics in atomically thin heterostructures, *Science* **366**, 870 (2019).
- [6] P. Merkl, F. Mooshammer, P. Steinleitner, A. Girnghuber, K. Q. Lin, P. Nagler, J. Holler, C. Schüller, J. M. Lupton, T. Korn, S. Ovesen, S. Brem, E. Malic, and R. Huber, Ultrafast transition between exciton phases in van der Waals heterostructures, *Nature Mater.* **18**, 691 (2019).
- [7] D. Schmitt, J. P. Bange, W. Bennecke, A. AlMutairi, G. Meneghini, K. Watanabe, T. Taniguchi, D. Steil, D. R. Luke, R. T. Weitz, S. Steil, G. S. M. Jansen, S. Brem, E. Malic, S. Hofmann, M. Reutzler, and S. Mathias, Formation of moiré interlayer excitons in space and time, *Nature (London)* **608**, 499 (2022).
- [8] O. Karni, E. Barré, V. Pareek, J. D. Georganas, M. K. L. Man, C. Sahoo, D. R. Bacon, X. Zhu, H. B. Ribeiro, A. L. O'Beirne, J. Hu, A. Al-Mahboob, M. M. M. Abdelrasoul, N. S. Chan, A. Karmakar, A. J. Winchester, B. Kim, K. Watanabe, T. Taniguchi, K. Barmak, F. H. da Jornada *et al.*, Structure of the moiré exciton captured by imaging its electron and hole, *Nature (London)* **603**, 247 (2022).
- [9] M. Förg, L. Colombier, R. K. Patel, J. Lindlau, A. D. Mohite, H. Yamaguchi, M. M. Glazov, D. Hunger, and A. Högele, Cavity-control of interlayer excitons in van der Waals heterostructures, *Nature Commun.* **10**, 3697 (2019).
- [10] S. Kundu, T. Amit, H. Krishnamurthy, M. Jain, and S. Refaely-Abramson, Exciton fine structure in twisted transition metal dichalcogenide heterostructures, *npj Comput. Mater* **9**, 186 (2023).
- [11] E. Barré, O. Karni, E. Liu, A. L. O'Beirne, X. Chen, H. B. Ribeiro, L. Yu, B. Kim, K. Watanabe, T. Taniguchi, K. Barmak, C. H. Lui, S. Refaely-Abramson, F. H. da Jornada, and T. F. Heinz, Optical absorption of interlayer excitons in transition-metal dichalcogenide heterostructures, *Science* **376**, 406 (2022).
- [12] M. H. Naik, E. C. Regan, Z. Zhang, Y.-H. Chan, Z. Li, D. Wang, Y. Yoon, C. S. Ong, W. Zhao, S. Zhao, M. I. B. Utama, B. Gao, X. Wei, M. Sayyad, K. Yumigeta, K. Watanabe, T. Taniguchi, S. Tongay, F. H. da Jornada, F. Wang, and S. G. Louie, Intralayer charge-transfer Moiré excitons in van der Waals superlattices, *Nature (London)* **609**, 52 (2022).
- [13] A. Sood, J. B. Haber, J. Carlström, E. A. Peterson, E. Barre, J. D. Georganas, A. H. Reid, X. Shen, M. E. Zajac, E. C. Regan, J. Yang, T. Taniguchi, K. Watanabe, F. Wang, X. Wang, J. B. Neaton, T. F. Heinz, A. M. Lindenberg, F. H. da Jornada, and A. Raja, Bidirectional phonon emission in two-dimensional heterostructures triggered by ultrafast charge transfer, *Nature Nanotechnol.* **18**, 29 (2023).
- [14] M. Fogler, L. Butov, and K. Novoselov, High-temperature superfluidity with indirect excitons in van der Waals heterostructures, *Nature Commun.* **5**, 4555 (2014).
- [15] Z. Wang, D. A. Rhodes, K. Watanabe, T. Taniguchi, J. C. Hone, J. Shan, and K. F. Mak, Evidence of high-temperature exciton condensation in two-dimensional atomic double layers, *Nature (London)* **574**, 76 (2019).
- [16] L. Sigl, F. Sigger, F. Kronowetter, J. Kiemle, J. Klein, K. Watanabe, T. Taniguchi, J. J. Finley, U. Wurstbauer, and A. W. Holleitner, Signatures of a degenerate many-body state of interlayer excitons in a van der Waals heterostack, *Phys. Rev. Res.* **2**, 042044(R) (2020).

- [17] Y. Bai, S. Liu, Y. Guo, J. Pack, J. Wang, C. R. Dean, J. Hone, and X.-Y. Zhu, Evidence for exciton crystals in a 2d semiconductor heterotrilaier, *Nano Lett.* **23**, 11621 (2022).
- [18] Y. Slobodkin, Y. Mazuz-Harpaz, S. Refaely-Abramson, S. Gazit, H. Steinberg, and R. Rapaport, Quantum phase transitions of trilayer excitons in atomically thin heterostructures, *Phys. Rev. Lett.* **125**, 255301 (2020).
- [19] M. Troue, J. Figueiredo, L. Sigl, C. Paspalides, M. Katzer, T. Taniguchi, K. Watanabe, M. Selig, A. Knorr, U. Wurstbauer, and A. W. Holleitner, Extended Spatial Coherence of Interlayer Excitons in MoSe₂/WSe₂ Heterobilayers, *Phys. Rev. Lett.* **131**, 036902 (2023).
- [20] M. Katzer, M. Selig, L. Sigl, M. Troue, J. Figueiredo, J. Kiemle, F. Sigger, U. Wurstbauer, A. W. Holleitner, and A. Knorr, Exciton-phonon scattering: Competition between the bosonic and fermionic nature of bound electron-hole pairs, *Phys. Rev. B* **108**, L121102 (2023).
- [21] K. F. Mak and J. Shan, Opportunities and challenges of interlayer exciton control and manipulation, *Nature Nanotechnol.* **13**, 974 (2018).
- [22] D. M. Kennes, M. Claassen, L. Xian, A. Georges, A. J. Millis, J. Hone, C. R. Dean, D. Basov, A. N. Pasupathy, and A. Rubio, Moiré heterostructures as a condensed-matter quantum simulator, *Nature Phys.* **17**, 155 (2021).
- [23] M. S. Hybertsen and S. G. Louie, Electron correlation in semiconductors and insulators: Band gaps and quasiparticle energies, *Phys. Rev. B* **34**, 5390 (1986).
- [24] M. Rohlfing and S. G. Louie, Electron-hole excitations and optical spectra from first principles, *Phys. Rev. B* **62**, 4927 (2000); Electron-hole excitations in semiconductors and insulators, *Phys. Rev. Lett.* **81**, 2312 (1998).
- [25] S. G. Louie and A. Rubio, Quasiparticle and optical properties of solids and nanostructures: The GW-BSE approach, in *Handbook of Materials Modeling: Methods*, pp. 215–240 (Springer, Berlin, 2005).
- [26] S. G. Louie, Y.-H. Chan, F. H. da Jornada, Z. Li, and D. Y. Qiu, Discovering and understanding materials through computation, *Nature Mater.* **20**, 728 (2021).
- [27] D. Y. Qiu, T. Cao, and S. G. Louie, Nonanalyticity, valley quantum phases, and lightlike exciton dispersion in monolayer transition metal dichalcogenides: Theory and first-principles calculations, *Phys. Rev. Lett.* **115**, 176801 (2015).
- [28] P. Cudazzo, F. Sottile, A. Rubio, and M. Gatti, Exciton dispersion in molecular solids, *J. Phys.: Condens. Matter* **27**, 113204 (2015).
- [29] C. Attaccalite, M. Grüning, and A. Marini, Real-time approach to the optical properties of solids and nanostructures: Time-dependent bethe-salpeter equation, *Phys. Rev. B* **84**, 245110 (2011).
- [30] E. Perfetto, D. Sangalli, A. Marini, and G. Stefanucci, Nonequilibrium bethe-salpeter equation for transient photoabsorption spectroscopy, *Phys. Rev. B* **92**, 205304 (2015).
- [31] D. Sangalli, E. Perfetto, G. Stefanucci, and A. Marini, An ab-initio approach to describe coherent and non-coherent exciton dynamics, *Eur. Phys. J. B* **91**, 171 (2018).
- [32] Y.-H. Chan, D. Y. Qiu, F. H. da Jornada, and S. G. Louie, Giant exciton-enhanced shift currents and direct current conduction with subbandgap photo excitations produced by many-electron interactions, *Proc. Natl. Acad. Sci. USA* **118**, e1906938118 (2021).
- [33] D. Sangalli, Excitons and carriers in transient absorption and time-resolved arpes spectroscopy: An *ab initio* approach, *Phys. Rev. Mater.* **5**, 083803 (2021).
- [34] E. Perfetto and G. Stefanucci, Real-Time GW-Ehrenfest-Fan-Migdal Method for Nonequilibrium 2D Materials, *Nano Lett.* **23**, 7029 (2023).
- [35] G. Antonius and S. G. Louie, Theory of exciton-phonon coupling, *Phys. Rev. B* **105**, 085111 (2022).
- [36] H.-Y. Chen, D. Sangalli, and M. Bernardi, First-principles ultrafast exciton dynamics and time-domain spectroscopies: Dark-exciton mediated valley depolarization in monolayer WSe₂, *Phys. Rev. Res.* **4**, 043203 (2022).
- [37] Y.-H. Chan, J. B. Haber, M. H. Naik, J. B. Neaton, D. Y. Qiu, F. H. da Jornada, and S. G. Louie, Exciton lifetime and optical line width profile via exciton-phonon interactions: Theory and first-principles calculations for monolayer MoS₂, *Nano Lett.* **23**, 3971 (2023).
- [38] G. Cohen, J. B. Haber, J. B. Neaton, D. Y. Qiu, and S. Refaely-Abramson, [arXiv:2305.04223](https://arxiv.org/abs/2305.04223).
- [39] F. Paleari and A. Marini, Exciton-phonon interaction calls for a revision of the “exciton” concept, *Phys. Rev. B* **106**, 125403 (2022).
- [40] W. Kohn and L. J. Sham, Self-consistent equations including exchange and correlation effects, *Phys. Rev.* **140**, A1133 (1965).
- [41] D. Hernangómez-Pérez, A. Kleiner, and S. Refaely-Abramson, Reduced absorption due to defect-localized interlayer excitons in transition-metal dichalcogenide-graphene heterostructures, *Nano Lett.* **23**, 5995 (2023).
- [42] F. Giustino, Electron-phonon interactions from first principles, *Rev. Mod. Phys.* **89**, 015003 (2017).
- [43] See Supplemental Material at <http://link.aps.org/supplemental/10.1103/PhysRevB.108.L220305>. for more elaborate details about the computational method and computational details. The Supplemental Material also contains Refs. [54–61].
- [44] R. Rosati, R. C. Iotti, F. Dolcini, and F. Rossi, Derivation of nonlinear single-particle equations via many-body lindblad superoperators: A density-matrix approach, *Phys. Rev. B* **90**, 125140 (2014).
- [45] R. Rosati, F. Dolcini, and F. Rossi, Electron-phonon coupling in metallic carbon nanotubes: Dispersionless electron propagation despite dissipation, *Phys. Rev. B* **92**, 235423 (2015).
- [46] J. Xu, A. Habib, S. Kumar, F. Wu, R. Sundararaman, and Y. Ping, Spin-phonon relaxation from a universal *ab initio* density-matrix approach, *Nature Commun.* **11**, 2780 (2020).
- [47] E. Wietek, M. Florian, J. M. Göser, T. Taniguchi, K. Watanabe, A. Högele, M. M. Glazov, A. Steinhoff, and A. Chernikov, [arXiv:2306.12339](https://arxiv.org/abs/2306.12339).
- [48] M. M. Glazov, T. Amand, X. Marie, D. Lagarde, L. Bouet, and B. Urbaszek, Exciton fine structure and spin decoherence in monolayers of transition metal dichalcogenides, *Phys. Rev. B* **89**, 201302(R) (2014).
- [49] T. Deilmann, P. Krüger, and M. Rohlfing, Ab initio studies of exciton g factors: Monolayer transition metal dichalcogenides in magnetic fields, *Phys. Rev. Lett.* **124**, 226402 (2020).
- [50] T. Amit, D. Hernangómez-Pérez, G. Cohen, D. Y. Qiu, and S. Refaely-Abramson, Tunable magneto-optical properties in

- MoS₂ via defect-induced exciton transitions, *Phys. Rev. B* **106**, L161407 (2022).
- [51] A. Hötger, T. Amit, J. Klein, K. Barthelmi, T. Pelini, A. Delhomme, S. Rey, M. Potemski, C. Faugeras, G. Cohen, *et al.*, Spin-defect characteristics of single sulfur vacancies in monolayer mos2, *npj 2D Mater. Appl.* **7**, 30 (2023).
- [52] D. Y. Qiu, G. Cohen, D. Novichkova, and S. Refaely-Abramson, Signatures of dimensionality and symmetry in exciton band structure: Consequences for exciton dynamics and transport, *Nano Lett.* **21**, 7644 (2021).
- [53] F. Caruso, Nonequilibrium lattice dynamics in monolayer MoS₂, *J. Phys. Chem. Lett.* **12**, 1734 (2021).
- [54] D. Manzano, A short introduction to the lindblad master equation, *AIP Adv.* **10**, 025106 (2020).
- [55] J. Deslippe, G. Samsonidze, D. A. Strubbe, M. Jain, M. L. Cohen, and S. G. Louie, BerkeleyGW: A massively parallel computer package for the calculation of the quasiparticle and optical properties of materials and nanostructures, *Comput. Phys. Commun.* **183**, 1269 (2012).
- [56] M. J. van Setten, M. Giantomassi, E. Bousquet, M. J. Verstraete, D. R. Hamann, X. Gonze, and G.-M. Rignanese, The pseudodojo: Training and grading a 85 element optimized norm-conserving pseudopotential table, *Comput. Phys. Commun.* **226**, 39 (2018).
- [57] R. C. Iotti and F. Rossi, Energy dissipation and decoherence in solid-state quantum devices: Markovian versus non-Markovian treatments, *Entropy* **22**, 489 (2020).
- [58] F. H. da Jornada, D. Y. Qiu, and S. G. Louie, Nonuniform sampling schemes of the Brillouin zone for many-electron perturbation-theory calculations in reduced dimensionality, *Phys. Rev. B* **95**, 035109 (2017).
- [59] A. Tkatchenko and M. Scheffler, Accurate molecular van der Waals interactions from ground-state electron density and free-atom reference data, *Phys. Rev. Lett.* **102**, 073005 (2009).
- [60] J. P. Perdew, K. Burke, and M. Ernzerhof, Generalized gradient approximation made simple, *Phys. Rev. Lett.* **77**, 3865 (1996).
- [61] S. S. Poncé, E. R. Margine, C. Verdi, and F. Giustino, EPW: Electron-phonon coupling, transport and superconducting properties using maximally localized Wannier functions, *Comput. Phys. Commun.* **209**, 116 (2016).